combined polymer–solvent interactions are more favorable than either set singly and there is a minimization of the free energy when the mixed solvent has a specific composition.

We are continuing work in this area in order to provide further evidence in favor of this simple interpretation for cosolvency, which appears to depend largely on the enthalpic interactions associated with each system rather than entropic ones.

Registry No. Polystyrene (homopolymer), 9003-53-6; methylcyclopentane, 96-37-7; acetone, 67-64-1; diethyl ether, 60-29-7.

References and Notes

(1) Cowie, J. M. G., McEwen, I. J. *J. Chem. Soc., Faraday Trans. 1* 1974, *70*, 171.
(2) Cowie, J. M. G.; McEwen, I. J. *Polymer* 1983, *24*, 1449.
(3) Cowie, J. M. G.; McCrindle, J. T. *Eur. Polym. J.* 1972, *8*, 1325.
(4) Cowie, J. M. G.; McEwen, I. J. *Macromolecules* 1974, *7*, 291.
(5) Palit, S. R.; Colombo, G.; Mark, H. *J. Polym. Sci.* 1951, *6*, 295.
(6) Schuster, R. H.; Cantow, H.-J.; Klotz, S. *Polym. Bull.* 1982, *8*, 351.
(7) Horta, A.; Fernández-Pierola, I. *Macromolecules* 1981, *14*, 1519.
(8) Wolf, B. A.; Blaum, G. *J. Polym. Sci., Polym. Phys. Ed.* 1975, *13*, 1115.
(9) Wolf, B. A. *Makromol. Chem.* 1978, *179*, 2265.
(10) Scott, R. L. *J. Chem. Phys.* 1949, *17*, 268.
(11) Wolf, B. A.; Molinari, R. J. *Makromol. Chem.* 1973, *173*, 241.
(12) Patterson, D. *Macromolecules* 1969, *2*, 672.
(13) Siow, K. S.; Delmas, G.; Patterson, D. *Macromolecules* 1972, *5*, 29.
(14) Flory, P. J. *J. Am. Chem. Soc.* 1965, *87*, 1833.
(15) Cowie, J. M. G.; McEwen, I. J. *Polymer*, in press.
(16) Benson, G. C.; Singh, J. *J. Phys. Chem.* 1968, *72*, 1345.
(17) Sameshita, J. *J. Am. Chem. Soc.* 1918, *40*, 1482.
(18) Howell, P. J.; Skillerne de Bristowe, B. J.; Stubley, D. *J. Chem. Soc. A* 1971, 394.
(19) Cowie, J. M. G.; McEwen, I. J. *Polymer* 1975, *16*, 244.
(20) Cowie, J. M. G.; McEwen, I. J. *J. Chem. Soc., Faraday Trans.* 1976, *72*, 526.
(21) Timmermans, J. "Physico-chemical Constants of Pure Organic Compounds"; Elsevier: New York, 1980.
(22) Allen, G.; Gee, G.; Wilson, G. T. *Polymer*, 1960, *1*, 456.
(23) Patterson, D.; Bardin, J. *Polymer* 1969, *10*, 247.
(24) Flory, P. J.; Höcker, H.; Blake, G. J. *Trans. Faraday Soc.* 1971, *67* (8), 2251.

Dynamic Scattering from Bimodal Polymer Solutions. 1. Apparent Diffusion Coefficient

A. Ziya Akcasu* and Boualem Hammouda

Department of Nuclear Engineering, The University of Michigan, Ann Arbor, Michigan 48109

Timothy P. Lodge† and Charles C. Han

Center for Material Science, The National Bureau of Standards, Washington, D.C. 20234. Received May 17, 1983

ABSTRACT: The dynamic scattering matrix **S**(q,t) for scattering from multimodal systems is formulated, and explicit results in the case of bimodal systems are presented in the small-q limit. The total dynamic scattering function is expressed in this limit as a weighted sum of two exponentials with decay rates Γ_1 and Γ_2. Both the decay rates and the weighting factors are calculated in terms of the concentrations and molecular weights of the two components. The dependence of the apparent diffusion coefficient D_{app} on the concentrations of both components is calculated, and the results are compared to experimental data for polystyrene ($M_w = 1.79 \times 10^5$ and 1.05×10^6) in cyclohexane at the Θ point. The magnitude of the interference effect on the concentration dependence of D_{app} is studied quantitatively. The concentration dependence of the apparent diffusion coefficient and the collective diffusion coefficient in a single-component system is expressed in terms of the pair correlation function for polymer molecules.

Introduction

The purpose of this paper is to investigate dynamic scattering from polydisperse polymer solutions and to provide tractable theoretical formulas to interpret quantities that can be extracted from the scattering data with sufficient precision, such as the apparent diffusion coefficient and the decay rates of the scattering function. Specifically, we consider a solution containing chemically identical polymers with different molecular weights. The continuous molecular weight distribution is assumed to be lumped into groups such that N_g is the number of polymers with molecular weights in a narrow interval ΔM about M_g. The number of groups G is not restricted. In the small-q region where $qR_G \ll 1$ is satisfied in all groups, the measured dynamic scattering function $S(q,t)$ can be represented as

$$S(q,t) = S(q) \sum_{g=1}^{G} A_g \exp(-\Gamma_g t) \qquad (1)$$

where $S(q)$ is the static structure factor. The coefficients A_g and the decay rates Γ_g are determined experimentally by appropriate data analysis such as the histogram technique[1,2] or least-squares curve fitting. In the zero-concentration limit, $\Gamma_g \rightarrow q^2 D_g$, where D_g is the translational diffusion coefficient of an isolated polymer with molecular weight M_g, and

$$A_g = C_g M_g / \sum_{g=1}^{G} C_g M_g \qquad (2)$$

where C_g is the mass concentration of the polymers in the gth group.

At finite concentrations, the above simple interpretation of $S(q,t)$ based on linear superposition is no longer strictly valid due to the interference effects among different components. For example, $q^{-2}\Gamma_g$ can no longer be identified

†Present address: Department of Chemistry, University of Minnesota, Minneapolis, MN 55455.

as the concentration-dependent collective diffusion coefficient of polymers with molecular weight M_g alone, as assumed in the study of polydispersity with histogram analysis.[1,2] It depends, in general, on the concentrations and molecular weights of all the other components in the solution, as is also the case for the expansion coefficients A_g. Caroline,[3,4] who first pointed out the inadequacy of the above interpretation of the decay rates obtained by the histogram technique, suggested a dependence of each decay constant on the total concentration and proposed a form of coupling between different molecular weights. The main motivation of this work is a quantitative investigation of the interference effects on the decay rates as well as on the expansion coefficients, by studying dynamic scattering from bimodal solutions containing two components with widely separated molecular weights. The present paper is devoted to the calculation of the apparent diffusion coefficient as a function of the total concentration of polymers and the ratio of concentrations of the two components. The theoretical predictions are compared with experimental results obtained either by forcing the measured $S(q,t)$ from a bimodal solution to fit a single exponential or by extracting the first cumulant through a cumulant analysis. The investigation of the variation of the individual decay constants Γ_1 and Γ_2 and expansion coefficients A_1 and A_2 with the concentrations of the two components will be presented in a future publication after detailed experimental data become available. However, the general theory of dynamic scattering from bimodal systems is included in this paper.

Dynamic Scattering from Multicomponent Systems

In this section, we present the formal theory of dynamic scattering from polymer solutions containing an arbitrary number of components. For simplicity the formalism will be developed first in the case of a bimodal solution (with components A and B); these results can be extended to multimodal systems.

We denote the scattering length densities of an A component in the Fourier space by $\rho_A(\mathbf{q})$; viz.

$$\rho_A(\mathbf{q}) = \sum_{\alpha=1}^{N_A} \rho_{A\alpha}(\mathbf{q})e^{i\mathbf{q}\cdot\mathbf{R}_\alpha}$$

and

$$\rho_{A\alpha}(\mathbf{q}) = \sum_{j=1}^{n_A} a_{\alpha j}{}^A \exp(i\mathbf{q}\cdot\mathbf{S}_{\alpha j}) \tag{3}$$

where N_A and n_A are the number of polymers of kind A in the solution and the number of monomers in such an A molecule, respectively. $\mathbf{R}_\alpha$ denotes the position of the center of mass of the αth polymer. $\mathbf{S}_{\alpha j}$ and $a_{\alpha j}{}^A$ denote the position of the jth monomer about the center of mass and its scattering length, respectively. We introduce the column vector $\rho(\mathbf{q}) = [\rho_A(\mathbf{q}),\rho_B(\mathbf{q})]^T$ and the associated dynamic correlation matrix $\mathbf{S}(\mathbf{q},t)$ by

$$\mathbf{S}(q,t) = \langle \rho(\mathbf{q})\rho^+(\mathbf{q},t)\rangle \tag{4}$$

where $\rho^+(\mathbf{q},t)$ is the adjoint row vector. In vector notation, the formalism is not restricted to two components only. The time dependence of $\rho(t)$ (we suppress the $\mathbf{q}$ dependence unless needed explicitly) is assumed to be given by

$$d\rho(t)/dt = -\mathcal{L}\rho(t) \tag{5}$$

where $\mathcal{L}$ is a linear, time-independent operator, e.g., the adjoint of the Kirkwood–Riseman diffusion operator, operating on the position vectors of all the monomers. With the usual projection operator technique of Zwanzig[5,6] and

Mori,[7] one obtains[8] an exact equation for $\mathbf{S}(t)$:

$$d\mathbf{S}(t)/dt = -\Omega\cdot\mathbf{S}(t) + \int_0^t du\ \Phi(u)\cdot\mathbf{S}(t-u) \tag{6}$$

The relaxation matrix Ω is defined by

$$\Omega(q) = \langle\rho\mathcal{L}\rho^+\rangle\cdot\langle\rho\rho^+\rangle^{-1} \tag{7}$$

where $\langle[...]\rangle$ denotes the equilibrium average of the quantity $[...]$. We assume that $\mathcal{L}$ is self-adjoint in the sense that $\langle A(\mathcal{L}B)^*\rangle = \langle(\mathcal{L}A)B^*\rangle$ for any two functions of monomer positions. The last matrix in eq 7 is the inverse of the static structure matrix $\mathbf{S}(q) = \langle\rho\rho^+\rangle$. The memory matrix $\Phi(q,t)$ has its usual definition:

$$\Phi(t) = \langle\mathbf{f}(t)\cdot\mathbf{f}^+(0)\rangle\cdot\langle\rho\rho^+\rangle^{-1} \tag{8}$$

where the random force denotes

$$\mathbf{f}(t) = \exp[-(1-\mathcal{P})t\mathcal{L}](1-\mathcal{P})\mathcal{L}\rho$$

The projection operator $\mathcal{P}$ projects an arbitrary function G of positions onto the initial-state vector $\rho(q)$:

$$\mathcal{P}G = \langle G\rho^+\rangle\cdot\langle\rho\rho^+\rangle^{-1}\cdot\rho$$

Equation 6 can be solved with Laplace transforms as

$$\tilde{\mathbf{S}}(s) = \tilde{\mathbf{M}}(s)\cdot\mathbf{S}(t=0) \tag{9a}$$

where

$$\tilde{\mathbf{M}}(s) = [s\mathbf{I} + \Omega - \tilde{\Phi}(s)]^{-1} \tag{9b}$$

In a dynamic scattering experiment, one measures the total dynamic scattering function

$$S(t) = \langle\rho(0)\rho^*(t)\rangle \tag{10}$$

where $\rho = \mathbf{E}^T\rho$, with $\mathbf{E} = \text{col}\ [1, ..., 1]$, denotes the total density of scattering centers in the solution. Combining (9) and (10), we obtain an exact expression for $S(t)$ as

$$S(t) = \mathbf{E}^T\mathbf{M}(t)\mathbf{S}(0)\mathbf{E} \tag{11}$$

where $\mathbf{M}(t)$ is the inverse Laplace transform $\tilde{\mathbf{M}}(s)$. This formal result is a convenient starting point for the investigation of the time behavior of $S(q,t)$, the first cumulant, and the apparent diffusion coefficient. The time dependence of $S(q,t)$ for values of q satisfying $qR_G \ll 1$ can be studied by considering the Markov limit of (6), in which $q \rightarrow 0$ and $t \rightarrow \infty$ with q^2t constant. This limit is equivalent to replacing $\tilde{\Phi}(s)$ in (9b) by $\tilde{\Phi}(s=0)$ provided it exists. Then the inverse Laplace transform of $\tilde{\mathbf{M}}(s)$ yields

$$\mathbf{M}(t) = \exp(-\Lambda t) \tag{12}$$

where the relaxation matrix $\Lambda(q)$ is defined by

$$\Lambda(q) = q^2 \lim_{q\to 0} \frac{1}{q^2}\left[\Omega(q) + \int_0^\infty dt\ \Phi(q,t)\right] \tag{13}$$

It is known that $\mathbf{M}(t)$ can be expanded as

$$\mathbf{M}(t) = \sum_{j=1}^G e^{-\Gamma_j t}\mathbf{m}_j \tag{14}$$

where $\Gamma_j, j = 1, ..., G$, are the eigenvalues of the Hermitian matrix Λ. The idempotent matrices that satisfy $\mathbf{m}_j\mathbf{m}_k = \delta_{jk}\mathbf{m}_k$ are defined by $\mathbf{m}_j = \mathbf{Q}\mathbf{d}_j\mathbf{Q}^{-1}$, where $\mathbf{d}_j$ is a matrix with all elements equal to zero except the jth diagonal element, which is equal to 1. The square matrix $\mathbf{Q}$ diagonalizes Λ by the similarity transformation $\mathbf{Q}^{-1}\Lambda\mathbf{Q} = \text{diag}\ [\Gamma_1, ..., \Gamma_G]$. Using (14) in (11), we obtain the following expression for the dynamic scattering function $S(t)$:

$$S(t) = S(0)\sum_{j=1}^G A_j e^{-\Gamma_j t} \tag{15}$$

where

$$A_j = \frac{\mathbf{E}^T \mathbf{m}_j \mathbf{S}(0)\mathbf{E}}{S(0)} \tag{16}$$

These equations provide formally exact definitions of the decay rates Γ_j and the expansion coefficients A_j that can be used to investigate the interference effects on the decay constants at finite concentrations mentioned in the Introduction. This formalism allows the study of scattering from multimodal systems in which some or all of the monomers of each component are labeled by setting the scattering lengths $a_{\alpha j}{}^g$ equal to zero for the unlabeled monomers. We choose $a_{\alpha j}{}^g = 1$ everywhere since we are mainly concerned with the interpretation of light scattering experiments.

We present the results explicitly for a bimodal solution ($G = 2$):

$$A_1 = [\Gamma_1 + FS^{-1}]/(\Gamma_1 - \Gamma_2) \tag{17}$$

$$A_2 = [\Gamma_2 + FS^{-1}]/(\Gamma_2 - \Gamma_1) \tag{18}$$

where

$$F = (S_{AA} + S_{AB})(\Lambda_{BA} - \Lambda_{BB}) + (S_{BB} + S_{BA})(\Lambda_{AB} - \Lambda_{AA}) \tag{19}$$

The eigenvalues Γ_1 and Γ_2 are the roots of the quadratic equation

$$\Gamma^2 - 2\Lambda_{av}\Gamma - \Delta = 0 \tag{20}$$

where

$$\Lambda_{av} = \tfrac{1}{2}(\Lambda_{AA} + \Lambda_{BB})$$

$$\Delta = \Lambda_{AA}\Lambda_{BB} - \Lambda_{AB}\Lambda_{BA}$$

and are given by

$$\Gamma_{1,2} = \Lambda_{av} \pm (\Lambda_{av}{}^2 - \Delta^2)^{1/2} \tag{21}$$

In these equations the two components of the bimodal solution are identified by the subscripts A and B. Λ_{AA}, Λ_{AB}, Λ_{BA}, and Λ_{BB} are the matrix elements of the 2×2 relaxation matrix Λ introduced in (13). S in (18) is the total static structure factor, given by $S = S_{AA} + S_{AB} + S_{BA} + S_{BB}$, where $S_{AB} = \langle \rho_A \mathcal{L} \rho_B{}^* \rangle$.

The apparent diffusion coefficient is defined as the initial slope of $S(t)/S(0)$ after the Markov limit has been taken

$$D_{app} = \frac{1}{q^2} \sum_{j=1}^{G} \Gamma_j A_j \tag{22}$$

The following section presents an approximate calculation of D_{app} as a function of concentration and molecular weight of the components in bimodal solutions.

Apparent Diffusion Coefficient

The apparent diffusion coefficient defined in (22) corresponds to the long-time diffusion coefficient since it is calculated from the initial slope of $S(q,t)/S(q,0)$ after the Markov limit has been taken. We can define the short-time diffusion coefficient in an analogous manner to the diffusion coefficient in single-component solutions by starting from the short-time behavior of $\mathbf{S}(q,t)$ in (6) at a fixed q, i.e.

$$\mathbf{S}(q,t) = \exp[-\Omega(q)t]\mathbf{S}(q,0) \tag{23}$$

and then calculating the initial slope of $S(q,t) = \mathbf{E}^T \mathbf{S}(q,t)\mathbf{E}$. The result can be expressed as

$$D_{app} = \lim_{q \to 0} \frac{1}{q^2} \frac{\mathbf{E}^T \mathbf{\Omega} \mathbf{S}(0)\mathbf{E}}{S(0)} \tag{24}$$

Using the definition of Ω in (7), it is easy to show that $\mathbf{E}^T \mathbf{\Omega} \mathbf{S}(0)\mathbf{E} = \langle \rho \mathcal{L} \rho^* \rangle$, so that the short-time diffusion coefficient can also be expressed as

$$D_{app} = \lim_{q \to 0} (\Omega(q)/q^2) \tag{25}$$

where $\Omega(q)$ is the usual first cumulant $\langle \rho \mathcal{L} \rho^* \rangle / \langle \rho \rho^* \rangle$ for $S(q,t)$ appearing in the Akcasu–Gurol formalism.[8] It is clear that the above procedure is equivalent to ignoring the memory matrix in the defining expression for the relaxation matrix, eq 13. It has now been understood that the short-time diffusion coefficient does not take into account the deformation in the average shape of a macromolecule during its diffusion.[9-13] The difference between long- and short-time diffusion coefficients in one-component dilute solutions has been estimated by Fixman[11,12] to be about 8% when the nonpreaveraged Oseen tensor is used and 1.68% when the Oseen tensor is preaveraged.

In this section we calculate explicitly the short-time apparent diffusion coefficient using its definition in (25). The validity of the approximation made by identifying the measured apparent diffusion coefficient as the short-time diffusion coefficient depends on the q values and the time interval of the experiment. However, for low q values involved in light scattering experiments, the long-time diffusion coefficient should be a more realistic estimate of the measured diffusion coefficient. Equation 25 can be written as

$$D_{app} = k_B T \lim_{q \to 0} (\mu(q)/S(q)) \tag{26}$$

where $\mu(q)$ can be identified as a generalized mobility defined by

$$\mu(q) = \langle \rho \mathcal{L} \rho^* \rangle / q^2 k_B T \tag{27}$$

where $k_B T$ is the temperature in energy units. In bimodal solutions $\rho = \rho_A + \rho_B$ so that $S(q)$ and $\mu(q)$ are of the following form:

$$S = S_{AA} + S_{AB} + S_{BA} + S_{BB}$$

$$\mu = \mu_{AA} + \mu_{AB} + \mu_{BA} + \mu_{BB}$$

We first consider the calculation of $S_{AA}(q)$ and $S_{AB}(q)$. $S_{AA}(q)$ is defined explicitly by

$$S_{AA}(q) = N_A S_s{}^A(q) + N_A(N_A - 1)S_{int}{}^A(q) \tag{28a}$$

with

$$S_s{}^A(q) = \sum_{j,k}^{n_A} \langle \exp(i\mathbf{q} \cdot \mathbf{S}_{AjAk}) \rangle$$

$$S_{int}{}^A(q) = \sum_{j,k}^{n_A} \langle \exp[i\mathbf{q} \cdot (\mathbf{R}_{12} + \mathbf{S}_{1j2k})] \rangle$$

where $\mathbf{R}_{12}$ and $\mathbf{S}_{1j2k}$ refer to a pair of A molecules. On the other hand, $S_{AB}(q)$ for A $\neq$ B is defined by

$$S_{AB} = N_A N_B \sum_{j=1}^{n_A} \sum_{k=1}^{n_B} \langle \exp[i\mathbf{q} \cdot (\mathbf{R}_{AB} + \mathbf{S}_{AjBk})] \rangle \tag{28b}$$

The calculation of $S_{AA}(q)$ and $S_{AB}(q)$ in the small-q limit in terms of the second virial coefficient is well-known.[14] Here, we present only the results for both S_{AA} and S_{AB} in the following form:

$$S_{AB}(q \to 0) = N_A n_A{}^2 \delta_{AB} - 8N_B n_A n_B X_{AB}{}^3 C_A \tag{29a}$$

where the Kronecker delta δ_{AB} indicates that the first term

is present only in S_{AA} and S_{BB}. N_A and n_A are the number of polymers of component A and the number of monomers in each polymer of kind A, respectively. C_A is the concentration expressed as a volume fraction; i.e.

$$C_A = \frac{N_A}{V} \frac{4\pi}{3} (R_H{}^A)^3 \qquad (29b)$$

The hydrodynamic radius $R_H{}^A$ is defined by the Einstein–Stokes formula $R_H{}^A = k_B T / 6\pi\eta D_A$, where D_A is the diffusion coefficient of an isolated molecule of kind A. V in (29b) is the volume of the system. The parameter X_{AB} in (29a) is related to the second virial coefficient $A_2{}^{AB}$ by

$$X_{AB}{}^3 = \frac{M_A M_B}{N_{Av}(R_H{}^A)^3} \frac{3}{2\pi} A_2{}^{AB} \qquad (30)$$

where N_{Av} is Avogadro's number and M_A and M_B are the molecular weights. X_{AB} can also be expressed in terms of the pair distribution function $g_{AB}(R)$ for a pair of molecules of kind A and B as

$$X_{AB} = \bar{s}_{AB}/R_H{}^A \qquad (31a)$$

or

$$X_{AB}{}^3 = \left(\frac{R_G{}^A}{R_H{}^A}\right)^3 \frac{3}{8} \int_0^\infty dX \, X^2(1 - g_{AB}(X)) \quad (31b)$$

where X is the separation distance between the centers of masses of the two molecules normalized to the radius of gyration $R_G{}^A$ of an isolated A molecule. We note that $X_{BA} = (R_H{}^A/R_H{}^B)X_{AB}$. The physical meaning of $\bar{s}_{AA}$ follows from its definition in (31) with B = A, viz.

$$\frac{4\pi}{3}(2\bar{s}_{AA})^3 = \int d^3R \, [1 - g_{AA}(R)] \qquad (32)$$

as the radius of hard spheres with the same second virial coefficient as the polymers. It is a measure of the effective range of the excluded volume interaction. X_{AA} expresses this range relative to the hydrodynamic radius of a single molecule. We may relate X_{AA} to the interpenetration function Ψ_A as

$$X_{AA}{}^3 = \frac{3\pi^{1/2}}{4}\left(\frac{R_G{}^A}{R_H{}^A}\right)^3 \Psi_A \qquad (33)$$

using the definition of Ψ_A in terms of the second virial coefficient.[14] Since Ψ_A varies from zero at the Θ temperature to its asymptotic value 0.254 in the good solvent limit,[15] we find from (33) that the values of X_{AA} range from zero to approximately 1.297 between these limits. Here, we have taken into account the variation of the ratio R_H/R_G from 0.665 under Θ conditions[14] to 0.537 in the good solvent limit.[16] If $R_H/R_G = 0.665$ is also used in the latter limit, the limiting value of X_{AA} would be 1.047. The first estimate $X_{AA} = 1.297$ obtained with $R_H/R_G = 0.537$ seems somewhat larger than the reported experimental values in good solvents; e.g., $X_{AA} = 1.14$ for polystyrene ($M_w = 8.87 \times 10^5$) in toluene at 25 °C.[17] This may be due either to the fact that the asymptotic value $X_{AA} = 1.297$ has not been reached at these molecular weights or to the approximation involved in the fully swollen Gaussian model[16] used in the theoretical calculation of the limiting value 0.537 used for R_H/R_G.

The physical meaning of X_{AB} when A $\neq$ B can be discussed in a similar manner to that of X_{AA}. We shall return to this point later when we approximate X_{AB} in terms of X_{AA} and X_{BB}.

The total static structure factor is obtained in the small-q limit by summing S_{AB} in (28) as

$$S(q \to 0) =$$
$$N_A n_A{}^2[(1 - 8C_A X_{AA}{}^3) - 16x C_A X_{AB}{}^3 + xy(1 - 8C_B X_{BB}{}^3)] \qquad (34)$$

where we have used $S_{AB} = S_{BA}$ and introduced the molecular weight ratio $y = n_B/n_A$ and the mass concentration ratio $x = N_B n_B / N_A n_A$.

We now turn to the calculation of mobilities $\mu_{AB}(q)$ that are defined by

$$\mu_{AB}(q) = \langle \rho_A \mathcal{L} \rho_B{}^* \rangle / q^2 k_B T \qquad (35)$$

We are primarily interested in the small-q limit of μ_{AB}. Using the property of the operator $\mathcal{L}$, which is taken to be the adjoint of the Kirkwood–Riseman diffusion operator,[14] we can write $\mu_{AB}(q)$ as

$$\mu_{AB}(q) = \xi^{-1} \sum_{\alpha=1}^{N_A} \sum_{j=1}^{n_A} \sum_{\beta=1}^{N_B} \sum_{k=1}^{n_B} \langle H_{33}{}^{\alpha j, \beta k} \exp[i\mathbf{q}\cdot(\mathbf{R}_{\alpha\beta} + \mathbf{S}_{\alpha j\beta k})] \rangle$$
$$(36a)$$

where the z axis is chosen parallel to $\mathbf{q}$ and $\mathbf{H}^{\mu\nu} = \mathbf{H}(\mathbf{r}_{\mu\nu})$ is related to the Oseen tensor $\mathbf{T}$ by

$$\mathbf{H}^{\mu\nu} = \delta_{\mu\nu}\mathbf{I} + (1 - \delta_{\mu\nu})\xi\mathbf{T}^{\mu\nu} \qquad (36b)$$

ξ is the friction coefficient per monomer. H_{33} in (36a) denotes $\mathbf{q}\cdot\mathbf{H}\cdot\mathbf{q}/q^2$, and $\mathbf{r}_{\mu\nu}$ is the vector distance between any two monomers.

It is interesting to notice that the mobility can be expressed in terms of the static structure factor by first separating the diagonal part of $H_{33}{}^{\mu\mu} = 1$ in (36a) and then expressing $T_{33}(\mathbf{r})$ in terms of its Fourier transform $\tilde{T}_{33}(\mathbf{k})$:

$$\mu_{AA}(q) = \frac{N_A n_A}{\xi}\left(1 + \frac{\xi}{(2\pi)^3}\int d^3k \, \tilde{T}_{33}(\mathbf{q} - \mathbf{k}) \times \left[\frac{1}{N_A n_A} S_{AA}(\mathbf{k}) - 1\right]\right) \quad (37)$$

and when A $\neq$ B

$$\mu_{AB}(q) = \frac{1}{(2\pi)^3}\int d^3k \, \tilde{T}_{33}(\mathbf{q} - \mathbf{k})S_{AB}(\mathbf{k}) \qquad (38)$$

where $S_{AA}(q)$ and $S_{AB}(q)$ are defined in eq 28. Thus, the calculation of the mobilities can be reduced exactly to that of $S_{AA}(q)$ and $S_{AB}(q)$. The concentration dependences of $S(q)$ for all q and that of $\mu(q)$ in the small-q limit have been discussed previously in the case of single-component dilute solutions.[18] We extend these calculations here to bimodal systems starting from

$$\mu_{AA}(q) = \frac{N_A n_A}{\xi}\left(1 + \frac{\xi}{n_A}\sum_{j,k}^{n_A}\langle T_{33}(\mathbf{S}_{1j1k}) \exp(i\mathbf{q}\cdot\mathbf{S}_{1j1k})\rangle\right) +$$
$$N_A(N_A - 1)\sum_{j,k}^{n_A}\langle T_{33}(\mathbf{R}_{12} + \mathbf{S}_{1j2k}) \exp[i\mathbf{q}\cdot(\mathbf{R}_{12} + \mathbf{S}_{1j2k})]\rangle$$
$$(39)$$

and for A $\neq$ B

$$\mu_{AB}(q) =$$
$$N_A N_B \sum_j^{n_A}\sum_k^{n_B}\langle T_{33}(\mathbf{R}_{12} + \mathbf{S}_{1j2k}) \exp[i\mathbf{q}\cdot(\mathbf{R}_{12} + \mathbf{S}_{1j2k})]\rangle \quad (40)$$

which are obtained from (36) by splitting the summations over monomers into two parts: one over monomers belonging to the same chain, and one over monomers belonging to two different molecules.

The first term in (39) represents the q-dependent mobility of an isolated molecule of kind A, which we denote by $\mu_A(q)$. In the small-q limit it is related to the diffusion coefficient D_A as

$$\mu_A(q \to 0) = \frac{N_A n_A}{\xi}\left(1 + \frac{\xi}{n_A}\sum_{j,k}^{n_A}\langle T_{33}(\mathbf{S}_{1j1k})\rangle\right) =$$

$$\frac{N_A n_A^2}{k_B T}D_A = \frac{N_A n_A^2}{6\pi\eta R_H^A} \quad (41)$$

The second term in (39) and $\mu_{AB}(q)$ in (40) can be calculated approximately by resorting to the well-known single-contact approximation of Zimm[19] or to an approximation introduced by Akcasu and Benmouna[20] in which the vector distance belonging to two different molecules is replaced by the vector distance between the centers of masses of the molecules. This approximation is based on $|\mathbf{S}_{1j} - \mathbf{S}_{2k}| \ll |\mathbf{R}_{12}|$ and is expected to be valid in the good solvent limit, where the interpenetration of the molecules is not significant. Since it is already tested in the case of single-component systems,[21] we adopt this approximation in (39) and (40). Verifying first[22] that

$$\lim_{q\to0}\langle T_{33}(R_{AB})\exp(i\mathbf{q}\cdot\mathbf{R}_{AB})\rangle =$$

$$-\frac{2}{3\eta V}\int_0^\infty dR\,R[1 - g_{AB}(R)] \quad (42)$$

where $\tilde{T}_{33}(\mathbf{q}) = 0$ and the angular average $\langle T_{33}(\mathbf{R})\rangle = 1/(6\pi\eta R)$ has been used, one obtains both μ_{AA} and μ_{AB} as

$$\mu_{AB}(q\to0) = \mu_A[\delta_{AB} - 6C_A x Y_{AB}^2] \quad (43)$$

In (43), we have introduced

$$Y_{AB}^2 = \left(\frac{R_G^A}{R_H^A}\right)^2\frac{1}{2}\int_0^\infty dX\,X(1 - g_{AB}(X)) \quad (44)$$

where $X = R/R_G^A$. In order to attach a physical meaning to Y_{AA}, we evaluate this integral in (44) using a hard-sphere model for $g_{AA}(R)$ with a radius of $\bar{s}_{AA}$ introduced in (32) and find $Y_{AA} = X_{AA} = \bar{s}_{AA}/R_H^A$. This approximation was used by Akcasu and Benmouna[20] to express Y_{AA} in terms of the second virial coefficient that can be measured independently, in order to eliminate one unknown parameter in their calculations of the concentration dependence of the collective diffusion coefficient. Since $g_{AA}(X)$ is now available numerically through the two-chain Monte Carlo calculations by Olaj and co-workers,[23] we shall not approximate Y_{AA} by X_{AA}. One immediate difference between Y_{AA} and X_{AA} is that Y_{AA} is related to the first moment of the correlation function $[g_{AA}(X) - 1]$, whereas X_{AA} involves its second moment. Consequently, Y_{AA} remains finite at the Θ temperature even though X_{AA} vanishes by definition. We discuss the implications of this observation more in a later section.

Summing (43) on A and B, we obtain the total mobility in the small-q limit as

$$\mu(q\to0) =$$

$$\mu_A(1 - 6C_A x Y_{AA}^2) + \mu_B(1 - 6C_B x^{-1} Y_{BB}^2) - 12C_A x Y_{AB}^2\mu_A \quad (45)$$

where we have used the identity $Y_{BA} = (R_H^A/R_H^B)Y_{AB}$ that follows from the definitions of Y_{AB} and Y_{BA} and $g_{AB}(R) = g_{BA}(R)$.

It is important to note at this point that eq 45 displays only the explicit concentration dependence of $\mu(q\to0)$. In principle, both μ_A and μ_B, because they involve equilibrium averages with respect to the intramolecular segment distribution about the center of mass, depend implicitly on the concentrations of all components, due to the deformation of the intramolecular distribution of a chain experiencing a binary encounter with any other molecule. The concentration dependence of single-chain properties

Table I
Numerical Values for X_{AA} and Y_{AA}

| | 4-way | | 5-way | |
	Θ	good	Θ	good
I_1^{AA}	0.15	1.06	0.09	0.91
I_2^{AA}	$-0.024 \simeq 0$	1.27	$-0.04 \simeq 0$	1.06
X_{AA}	$-0.31 \simeq 0$	1.45^a	$-0.37 \simeq 0$	1.37^a
		1.16^b		1.11^b
Y_{AA}	0.41	1.36^a	0.32	1.26^a
		1.10^b		1.02^b

^{a} Calculated with $R_H/R_G = 0.537$. ^{b} Calculated with $R_H/R_G = 0.665$.

such as μ_A and μ_B was estimated earlier[18] in single-component systems and found to be small as compared to the explicit concentration dependence arising from the interference term. Therefore we ignore this effect in the present work.

Summary of the Analytical Results and Discussion

The apparent diffusion coefficient is obtained by substituting (34) and (45) into (26)

$$D_{app} =$$

$$\frac{D_A(1 - 6C_A Y_{AA}^2) + xyD_B(1 - 6C_B Y_{BB}^2) - 12xD_A C_A Y_{AB}^2}{1 + xy - 8X_{AA}^3 C_A - 8xyX_{BB}^3 C_B - 16xC_A X_{AB}^3} \quad (46)$$

To facilitate the comparison of this result with experiment, we summarize the definition of the symbols: D_A and D_B are the self-diffusion coefficients of the A and B molecules in the zero-concentration limit, and $y = M_B/M_A$ and $x = C_B^m/C_A^m$ are the molecular weight and mass concentration ratios of the components, respectively. C_A and C_B are the concentrations expressed as volume fractions as defined in (29b). The hydrodynamic radii R_H^A and R_H^B needed to calculate C_A and C_B are obtained from D_A and D_B via the Stokes–Einstein relation. Y_{AB} and X_{AB} are related (cf. eq 31 and 44) to the first and second moments of the pair correlation function, defined by

$$I_n^{AB} = \int_0^\infty dX\,X^n[1 - g_{AB}(X)] \quad (47)$$

In the case of identical molecules, $g_{AA}(X)$ has been computed by Olaj et al.[23] in the Θ and good solvent limits by Monte Carlo calculations with two chains of 50 steps each on 4- and 5-way cubic lattices. Using these data, we have calculated I_1^{AA}, I_2^{AA}, X_{AA}, and Y_{AA} in Table I. The numerical values in this table are to be considered only as crude estimates due to the numerical inaccuracies in the calculation of the moments in (47) with the trapezoidal rule, as well as the finite lengths of the chains in the Monte Carlo calculations. A nonzero value of the second moment under Θ conditions, proportional to the second virial coefficient, and the dependence of the results on the coordination number of the cubic lattice are probably indications of this inaccuracy. Direct evaluation of the moments through Monte Carlo calculations with longer chains as a function of chain length and temperature is needed for a more accurate theoretical prediction of the concentration dependence of chain properties in dilute solutions. However, the numbers in Table I show that the first moment I_1^{AA} is finite and positive at the Θ point, where I_2^{AA} is supposed to be zero, contrary to the conventional theoretical models[24] that imply $g_{AA}(X) = 1$ and, hence, $I_1^{AA} = I_2^{AA} = 0$ under Θ conditions. The fact that $I_1^{AA} > 0$, and hence, $Y_{AA}^2 > 0$, at least partially explains the predicted concentration dependence of the diffusion

coefficient at the Θ point as will be shown presently. Another observation from Table I is that Y_{AA} and X_{AA} tend to be almost equal numerically in the good solvent limit, as was assumed by Akcasu and Benmouna[20] on the basis of the hard-sphere model for g_{AA}.

Although the normalized moments $I_n{}^{AA}$ may still depend slightly on the molecular weight, especially in intermediate solvents, we treat them as constants and use $X_{AA} = X_{BB}$ and $Y_{AA} = Y_{BB}$ in the calculation of D_{app}.

The calculation of Y_{AB} and X_{AB} for two different chains directly from (47) is not possible because no computer data are yet available for $g_{AB}(X)$ when $n_A \neq n_B$. We can, however, relate them to Y_{AA} and X_{AA} approximately by treating A and B molecules as hard spheres with effective radii $\bar{s}_{AA}$ and $\bar{s}_{BB}$. Then $\bar{s}_{AB}$ becomes $(\bar{s}_{AA} + \bar{s}_{BB})/2$. This approximation leads to

$$X_{AB} = \frac{1}{2}[X_{AA} + (R_H{}^B/R_H{}^A)X_{BB}]$$

and

$$Y_{AB} = \frac{1}{2}[Y_{AA} + (R_H{}^B/R_H{}^A)Y_{BB}]$$

where $R_H{}^B/R_H{}^A = (n_B/n_A)^\nu$ with $\nu = 0.5$ and $\nu = 0.6$ in the Θ and good solvent limits. For intermediate solvents, such a power law does not apply. One may either use $R_H{}^B/R_H{}^A = D_A/D_B$ and calculate this ratio from the measured diffusion coefficients or resort to the calculations based on the blob hypothesis to calculate $R_H{}^A$ and $R_H{}^B$ as a function of temperature and molecular weight.[16,25,26]

We discuss certain limiting cases before we consider comparison with experimental results.

i. In the zero-concentration limit, (46) reduces to the expected result

$$D_{app}(0) = (D_A + xyD_B)/(1 + xy) \qquad (48)$$

ii. When the molecular weight of one component is much larger than the other, i.e., when $y \gg 1$, D_{app} reduces to the concentration-dependent diffusion coefficient of the larger molecule

$$D_B(C_B) = D_B[1 + k_D{}^B C_B]$$

where $k_D{}^B = 8X_{BB}{}^3 - 6Y_{BB}{}^2$.

iii. When the molecular weights of the A and B molecules are the same, one recaptures the single-component result

$$D(C) = D[1 + k_D C] \qquad (49)$$

where we have dropped the subscripts. C denotes the total concentration and k_D is defined by

$$k_D = 8X^3 - 6Y^2 \qquad (50)$$

In good solvents, $X \simeq Y$ as pointed out earlier, and (50) reduces to $k_D = X^2(8X - 6)$, which was obtained by Akcasu and Benmouna[20] for solutions away from the Θ point. Since X and Y are now available from two-chain Monte Carlo calculations, (50) extends the range of applicability of Akcasu and Benmouna's result. At the Θ point, where $X = 0$, $k_D = -6Y^2$, which leads to $k_D \simeq -1.00$ and $k_D \simeq -0.61$ in 4- and 5-way lattices when the Monte Carlo results are used. Since k_D is proportional to the first moment I_1 of $g(X) - 1$, which may be a slowly varying function of chain length, one may account for a possible molecular weight dependence of measured k_D values reported by Tsunashima et al.[27] It is interesting to compare (50) to $k_D = 3.2X^3 - 1$ in Yamakawa's treatment,[14] which implies $k_D = -1$ at the Θ temperature. This value represents a reference-frame correction in Yamakawa's theory and is essentially equal to the hydrodynamic volume fraction. The origin of the finite value of k_D under Θ conditions in

the fully statistical-mechanical approach based on Kirkwood–Risemann theory is entirely different.[22] It was shown[22] that there are two contributions to the concentration coefficients k_s of the friction coefficient (see eq 31 and 32 of the cited reference). The first, k_{s0}, is related to the first moment of the chain pair correlation function and equilibrium monomer distribution about the center of mass and becomes equal to $6Y^2$ when the molecules are treated as point particles; i.e., $R_G \rightarrow 0$. The second, k_{sc}, accounts for the deformation of the intramolecular segment distributions about the center of mass when two chains experience a binary encounter. In the classical theories of the second virial coefficient, such as the Flory–Krigbaum theory of pair interaction potential,[14] the pair correlation function vanishes identically at all separation distances at the Θ point, and consequently, $k_{s0} = 0$, as pointed out earlier. On the other hand, the Akcasu–Benmouna model,[20] which we have used in this paper for its simplicity, essentially ignores the internal structure of the chains and washes out the effects arising from the deformation of chains in a pair, which is more significant under Θ conditions, where the interpenetration of chains is more likely. Akcasu[22] attempted to estimate the magnitude of k_{sc} within the framework of classical theories, assuming that the deformation is spherical with an increase in the radius of gyration as a function of the separation distance $R_G(R)$. He concluded that the result is too sensitive to the model used for $R_G(R)$ to be conclusive, ranging from about -1 to -2. At present, it is not possible to see whether $k_s = k_{s0} + k_{sc}$ as calculated by Akcasu can alone account for the observed concentration dependence of the translational diffusion coefficient in Θ solvents. With the detailed information obtained recently by two-chain Monte Carlo calculations[23] on $g(R)$, hydrodynamic radius, and chain dimensions as a function of separation distance R, a more accurate estimate of k_s will be possible.

We conclude this discussion by noting that a reference-frame correction to the calculation of the diffusion coefficient through the first cumulant does not arise in the fully statistical-mechanical approach based on the conventional Kirkwood–Riseman theory of chain dynamics where monomers are treated as point particles without volume. Should this correction be needed to improve the agreement between theory and experiment, as concluded by Van den Berg and Jamieson,[21] then the necessary modifications will have to be made in the Kirkwood–Riseman diffusion equation in the statistical-mechanical approach. Alternatively, the correction term may be added to the final result as done in Yamakawa's theory and discussed in ref 21. It is, however, not clear to us at this stage whether this correction is needed when interpreting the diffusion coefficient that is inferred from the initial slope of the dynamic structure factor, which measures the correlation function of monomer density fluctuations at two space points in a fixed coordinate frame. We think that this point requires further attention.

iv. Under Θ conditions, (46) reduces with $X_{AA} = X_{AB} = 0$ and $Y_{AA} = Y_{BB}$ to

$$D_{app}(C) = D_{app}(0) \times$$

$$\left(1 - 6C_A Y_{AA} \frac{D_A + xyD_B\dfrac{C_B}{C_A} + xD_A\left[1 + \dfrac{R_H{}^B}{R_H{}^A}\right]}{D_A + xyD_B} \right) \qquad (51)$$

which is a function of Y_{AA}. In light of the previous discussions, we treat Y_{AA} as an adjustable parameter in (51),

Table II
Experimental and Theoretical Data for $D_{app} \times 10^{10}$ (cm²/s)

total concn, mg/mL	x = 0.1[a]			x = 0.2			x = 0.3		
	single-exponential fit	first-cumulant fit	theor	single-exponential fit	first-cumulant fit	theor	single-exponential fit	first-cumulant fit	theor
2	2736 ± 42	2865 ± 30	2588	2342 ± 40	2475 ± 38	2246	2059 ± 20	2129 ± 25	2049
4	2450 ± 33	2528 ± 38	2476	2150 ± 22	2225 ± 29	2137	1962 ± 18	2023 ± 26	1940
6	2354 ± 17	2419 ± 21	2364	2013 ± 16	2078 ± 25	2027	1875 ± 14	1925 ± 14	1831
8	2224 ± 39	2290 ± 28	2252	1949 ± 22	2002 ± 29	1917	1758 ± 18	1793 ± 13	1722
10	2131 ± 23	2184 ± 21	2140	1836 ± 20	1878 ± 17	1807	1683 ± 14	1711 ± 13	1613

[a] Concentration ratio.
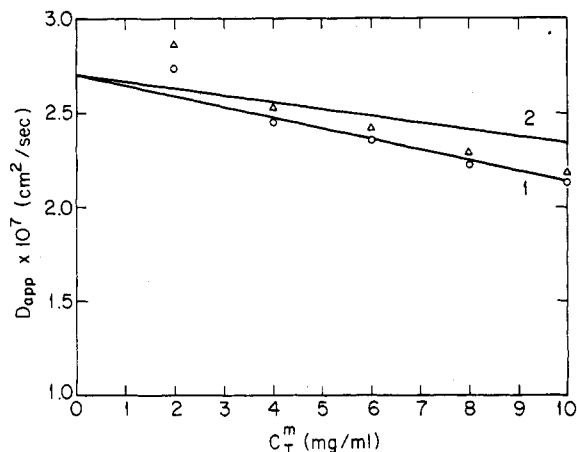
Figure 1. Variation of $D_{app} \times 10^7$ (cm²/s) as a function of the total concentration C_T^m, keeping the ratio of mass concentrations constant ($x = 0.1$). We have plotted the theoretical values with coupling between the two polymer components (curve 1) and without coupling (curve 2) and the experimental values using a single-exponential fit (O) and a first-cumulant fit (Δ).

Figure 2. Same as Figure 1 with $x = 0.2$.

Figure 3. Same as Figure 1 with $x = 0.3$.

investigate the variation of $D_{app}(C)$ with C_A and C_B, and compare the results to experiment.

Experiment in Θ Solvent

Monodisperse polystyrenes of $M_w = 1.05 \times 10^6$ (NBS-1479) and $M_w = 1.79 \times 10^5$ (NBS-705) in ACS spectrograde cyclohexane were used for the bimodal solutions. Three weight ratios x equal to 0.1, 0.2, and 0.3 of NBS-1479 (component B) to NBS-705 (component A) were used to prepare three sets of solutions. Five solutions with total polymer mass concentrations ($C_T^m = C_A^m + C_B^m$) of 2, 4, 6, 8, and 10 mg/mL were prepared volumetrically for each set by subsequent dilution of the most concentrated member of each set. All solutions were filtered directly into clean scattering cells through 0.45-μm Millipore filters, sealed, and stored at 40 °C until use.

All scattering data were obtained in the homodyne configuration using full photon-counting detection and a 128-channel correlator (Malvern 705). A Coherent Super-Graphite 4-W argon ion laser operated at 488 nm was used as the light source. The cylindrical sample cells were mounted in a bath of refractive index matching fluid. Temperature was maintained at 35.0 ± 0.1 °C, as determined by a copper–constantan thermocouple. Correlation data at seven different angles (25°, 27.5°, 30°, 32.5°, 35°, 37.5°, and 40°) were obtained and analyzed according to $C(q,t) = A + B \cdot (S(q,t))^2$, where B is an adjustable parameter and the base line A was also allowed to float. Two different procedures were used for this purpose. In the first procedure, a single-exponential function $e^{-\Omega t}$ was used to represent $S(q,t)$. In the second, a cumulant analysis was followed, and $S(q,t)$ was represented by $e^{-\Omega t(1+A_1 t)}$. The apparent diffusion coefficients in both cases were calculated from the nonlinear regression results of $\Omega(q)$, using $D_{app} = \Omega(q)/q^2$ and averaging over seven different q values. The single-exponential fit may be a better representation to the Markov limit correponding to the long-time diffusion coefficient while the first-cumulant results may be closer to the short-time diffusion coefficient. Since there is an estimated difference of
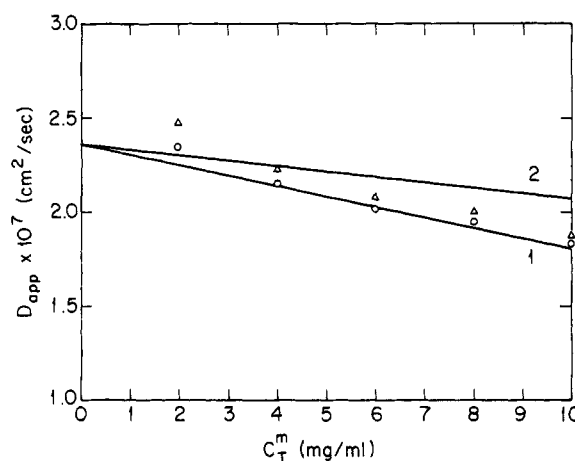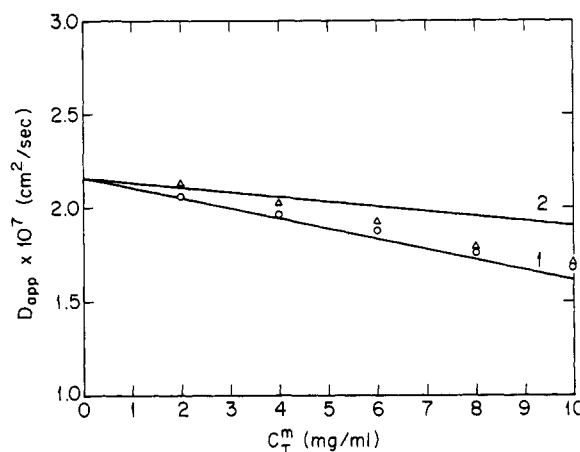
2–8% between the short- and long-time diffusion coefficients of a linear flexible chain, we include the results of both procedures. It is observed from the experimental results that D_{app} values obtained by cumulant analysis are consistently ~3% larger than those obtained by a single-exponential fit. Since we have used postulated forms for $S(q,t)$ (either single exponential or cumulant expansion) to extract D_{app}, we do not attach any quantitative significance to this difference of 3%. But it is consistent qualitatively with the theoretical trend that the short-time diffusion coefficient is larger than the long-time diffusion coefficient.

We analyzed the concentration dependence of the measured apparent diffusion coefficient using (51), taking $D_A = 3.45 \times 10^{-7}$ cm²/s for $M_w = 1.79 \times 10^5$ and $D_B = D_A(1.79/10.5)^{1/2}$ for $M_w = 1.05 \times 10^6$. We set $X_{AB}^2 = 0$ for both A = B and A ≠ B and choose $Y_{AA}^2 = 1.7$, which reproduces the experimental values for $x = 0.1$ (Figure 1). We should, however, mention that we are disregarding the first experimental point at $C_T^m = 0.2$ mg/mL in each case (too low a concentration to reliable). We notice that this same set of parameters gives a concentration dependence of D_{app} that agrees fairly well in the other cases ($x = 0.2$ and $x = 0.3$ in Figures 2 and 3, respectively). For each case, we are plotting in the same
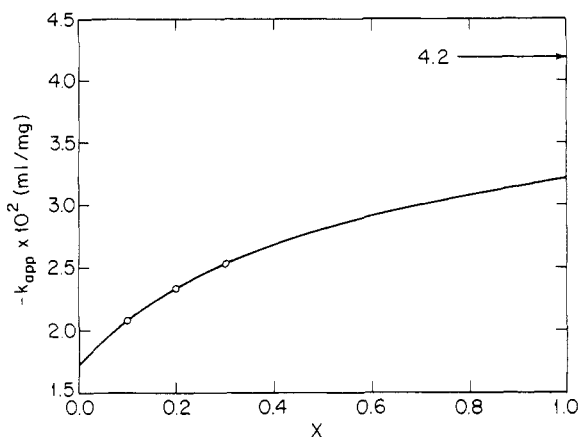
Figure 4. Variation of the slope, $-k_{app}$, of the apparent diffusion coefficient with the concentration ratio x. The points show the theoretical predictions at $x = 0.1$, 0.2, and 0.3 used in the experiments.

figure the concentration dependence of the apparent diffusion coefficient with and without coupling between different components (i.e., with and without the off-diagonal matrix elements S_{AB} and μ_{AB}) and the experimental data obtained from both the single-exponential fit and the first-cumulant fit.

We also plotted the variation of the slope k_{app} of the apparent diffusion coefficient with the concentration ratio x in Figure 4. $k_{app} = -1.7(4\pi/3)N_{Av}(R_H{}^A)^3/M_w{}^A = -0.017$ mL/mg when $x = 0$, i.e., when only A is present, and $k_{app} = -0.042$ mL/mg when $x = \infty$. When the total concentration is expressed in volume fraction as $C_T = C_A + C_B$, the new coefficient $k_{app}{}^v$ is -1.7 at $x = 0$, goes through a minimum of -1.88 for $x = 0.41$, and returns to -1.7 at $x = \infty$. This indicates, at least for these molecular weight ratios, that the concentration dependence of D_{app} mainly depends on total concentration in volume fraction and is insensitive to concentration ratio.

Concluding Remarks

In this paper, we have presented a general formalism to study the dynamic scattering matrix $\mathbf{S}(q,t)$ for scattering from multimodal systems using linear response theory and the projection operator technique. The formalism is exact and valid for all values of q. It shows that the total dynamic scattering function $S(q,t)$, equal to $\mathbf{E}^T \cdot \mathbf{S} \cdot \mathbf{E}$ in the small-q limit, may be expressed as a weighted sum of exponential functions with decay rates Γ_1, ..., Γ_n, which are the eigenfunctions of the $n \times n$ relaxation matrix, where n is the number of components in the system. The important conclusion is that Γ_j's are not the decay rates of the isolated individual components that depend on the molecular weight and concentration of a particular component, but rather they depend, as a result of interference effects in scattering, on the concentrations and molecular weights of all the other components as well. We have investigated the interference effect in detail by calculating the short-time apparent diffusion coefficient explicitly in the case of a bimodal system consisting of two chemically identical polymers with widely separated molecular

weights. The apparent diffusion coefficient has been inferred from the initial slope of the dynamic structure function measured by light scattering from bimodal solutions of polystyrene ($M_w = 1.79 \times 10^5$ and 1.05×10^6) in cyclohexane at 35.0 °C with four different values of total concentration and three different concentration ratios $x = C_B{}^m/C_A{}^m = 0.1$, 0.2, and 0.3. The slope of the apparent diffusion coefficient as a function of the total concentration k_{app} was -0.021, -0.023, and -0.025 mL/mg for $x = 0.1$, 0.2, and 0.3, respectively. By adjusting the value of $k_D = -6Y_{AA}{}^2$ to -1.7 to obtain the best fit to the data for $x = 0.1$, we obtained satisfactory agreement between the theory and experiment for the remaining cases. The value $k_D = -1.7$ is consistent with the measured concentration coefficient at the Θ temperature in single-component systems.[27] Theoretical results show that the interference effect accounts for about 35%, 48%, and 54% of the slope for the three concentration ratios.

References and Notes

(1) Gulari, E.; Gulari, E.; Tsunashima, Y.; Chu, B. *Polymer* **1979**, *20*, 347.
(2) Gulari, E.; Gulari, E.; Tsunashima, Y.; Chu, B. *Polymer* **1982**, *23*, 649.
(3) Caroline, D. *Polymer* **1981**, *22*, 576.
(4) Caroline, D. *Polymer* **1982**, *23*, 492.
(5) Zwanzig, R. *J. Chem. Phys.* **1960**, *33*, 338.
(6) Zwanzig, R. In *Lect. Theor. Phys.* **1961**, *3*, 106–141.
(7) Mori, H. *Prog. Theor. Phys.* **1965**, *33*, 423.
(8) Akcasu, A. Z.; Gurol, H. *J. Polym. Sci., Polym. Phys. Ed.* **1976**, *14*, 1.
(9) Dubois-Violette, E.; de Gennes, P.-G. *Physics* **1967**, *3*, 181.
(10) Mansfield, M. L. Dissertation, Dartmouth College, Hanover, NH, 1980.
(11) Fixman, M. *Macromolecules* **1981**, *14*, 1706, 1710.
(12) Fixman, M. *J. Chem. Phys.* **1965**, *42*, 3831.
(13) Akcasu, A. Z. *Macromolecules* **1982**, *15*, 1321.
(14) Yamakawa, H. "Modern Theory of Polymer Solutions"; Harper and Row: New York, 1971.
(15) Freed, K. F. *J. Phys. A* **1982**, *15*, 1931.
(16) Benmouna, M.; Akcasu, A. Z. *Macromolecules* **1978**, *11*, 1187.
(17) Han, C. C.; Akcasu, A. Z. *Polymer* **1981**, *22*, 1165.
(18) Akcasu, A. Z.; Hammouda, B. *Macromolecules* **1983**, *16*, 951.
(19) Zimm, B. H. *J. Chem. Phys.* **1946**, *14*, 164; **1948**, *16*, 1093.
(20) Akcasu, A. Z.; Benmouna, M. *Macromolecules* **1978**, *11*, 1193.
(21) Van den Berg, H.; Jamieson, A. M., to appear in *J. Polym. Sci., Polym. Phys. Ed.*
(22) Akcasu, A. Z. *Polymer* **1981**, *22*, 1169.
(23) Olaj, O. F.; Lantschbauer, N.; Pelinka, K. H. *Macromolecules* **1980**, *13*, 299.
(24) Flory, P. J.; Krigbaum, W. R. *J. Chem. Phys.* **1950**, *18*, 1086.
(25) Weill, G.; des Cloiseaux, J. *Physics* **1979**, *40*, 99.
(26) Daoud, M. Thesis, Université de Paris, 1977.
(27) Tsunashima, Y.; Nemoto, N.; Kurata, M. *Macromolecules* **1983**, *16*, 1184.